Available online at www.sciencedirect.com

SciVerse ScienceDirect

Ceramics International 38 (2012) 5643–5649

CERAMICS INTERNATIONAL

www.elsevier.com/locate/ceramint

Corrosion of oxide bonded silicon carbide refractories by molten salts in solid waste-to-energy facilities

P. Prigent [a], M.L. Bouchetou [a], J. Poirier [a,*], E. de Bilbao [a], E. Blond [b]

[a] CEMHTI – Conditions Extrêmes et Matériaux Haute Température et Irradiation, 1D, avenue de la Recherche Scientifique, 45071 Orléans, Cedex 2, France
[b] PRISME EA4229, Polytech'Orléans, Université d'Orléans, 8 rue L. de Vinci, 45072 Orléans, France

Received 3 March 2012; accepted 2 April 2012
Available online 11 April 2012

Abstract

Oxide bonded silicon carbide refractories are used successfully in solid waste-to-energy facilities (WtE). They are submitted to severe thermo-chemical stresses that limit their performance. Even if the corrosion resistance of silicon carbide is high, wear and failure of refractory lining are currently observed.

For a better understanding of corrosion mechanisms, oxide bonded silicon carbide refractories, collected in the combustion chamber of several WtE facilities, were examined. The main mechanisms of corrosion, according to the environment of refractories, were determined. The chemical composition and the nature of the corrosive agents were calculated from the thermo-chemical modeling. They are mainly condensed phases of sulfates and chlorides ($CaSO_4$, K_2SO_4, Na_2SO_4, KCl, and NaCl). In service conditions, these molten salts react with the SiC aggregates and the matrix of the refractories to form low melting compounds.

The post-mortem analyses showed the formation of para-wollastonite in the porosity and around the SiC grains, on the hot face of refractory tiles. Other phases such as cristobalite and microline ($KAlSiO_8$) were also formed down to the core of refractories. The volume expansion created by the formation of new mineral phases (cristobalite, para-wollastonite) causes the formation of micro cracks in the refractory lining.

In this paper, the degradation mechanisms of oxide bonded silicon carbide refractories are presented and the main research developments for the future are discussed.

Keywords: B. Microstructure-final; C. Corrosion; D. SiC; E. Refractories; Thermodynamic simulation

1. Introduction

The combustion chambers of municipal solid waste-to-energy facilities (WtE) are currently made of shaped silicon carbide tiles in order to promote thermal transfer from flue-gas and to protect the waterwall boiler tubes in which high pressure water is heated to produce steam and then electricity by means of turbines.

The wear of SiC refractory lining is a complex phenomenon due to the combined effects of thermal stress caused by temperature fluctuations, thermal gradient and chemical corrosion, thereby limiting its performance [1,2].

Combustion of municipal solid waste generates high temperature flue-gas ($T_{\text{flue-gas}} \sim 1200\ ^\circ\text{C}$) containing highly corrosive species as gases, particles or flying ashes [3,4] which play a major role in the corrosion of the refractory lining [5]. These compounds, in most cases chloride and sulfate species, react with the refractory lining.

The inorganic compounds, in most cases molten salts, oxides and alkali chlorides, condense and react with the refractory [6–8]. In this study, post mortem examinations of oxide bonded silicon carbide refractories have been performed after more than 8000 h of industrial operating conditions using dilatometry, X-ray diffraction (XRD) measurements and scanning electron microscopy (SEM) including chemical analysis by energy-dispersive X-ray spectroscopy (EDS).

Furthermore, thermodynamic equilibrium calculations have been performed, at service temperature, using the integrated thermodynamic database FactSage© in order to predict the

* Corresponding author at: CNRS-CEMHTI, 1D, avenue de la Recherche Scientifique, 45071 Orléans Cedex 2, France. Tel.: +33 2 38 25 55 14; fax: +33 2 38 63 81 03.
E-mail address: jacques.poirier@univ-orleans.fr (J. Poirier).

0272-8842/$36.00
http://dx.doi.org/10.1016/j.ceramint.2012.04.007

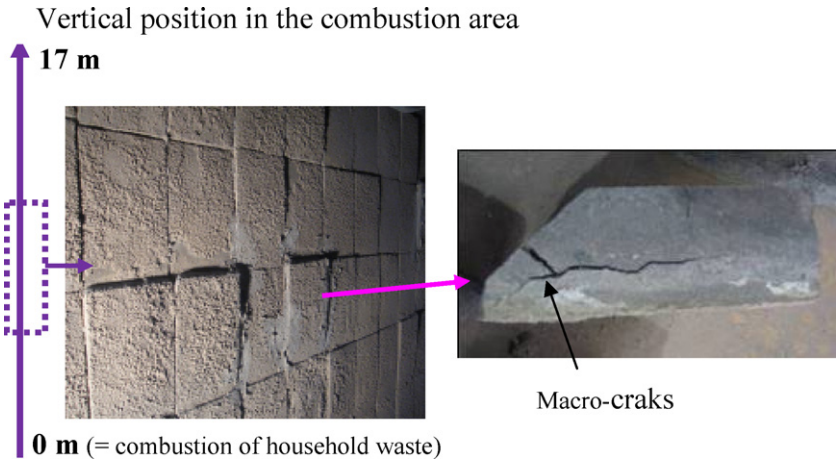

Fig. 1. Observation zone for the post-mortem study.

nature of the corrosive species generated by combustion and their thermochemical reactions with the refractory lining.

The purpose of this paper is to improve our comprehension of the corrosion mechanisms of the refractory lining and to propose recommendations.

2. Post-mortem examination

Tiles composed of SiC (90 wt%) with an alumino-silicate matrix are commonly used in combustion chamber of incinerator plants. Table 1 gives the typical properties of these SiC tiles.

Representative samples (several samples in various industrial sites) of SiC refractories, with a bonding phase composed of silico-aluminate oxides, were collected after more than 8000 h of industrial operating conditions. Cracks (Fig. 1) and a volume expansion (Fig. 2) due to corrosion were observed on the hot face of refractory tiles leading to the apparition of progressive bulge especially at a height between 4 and 10 m from the combustion area (Fig. 1). Thus, post-mortem observations were focused only on this area.

Fig. 2 shows a cross section of a corroded tile. A 3% difference in length expansion was measured between the hot face (corroded part) and the cold face (uncorroded part). A dilatometry, performed on an uncorroded tile shows a linear and regular reversible expansion (Fig. 3). On the other hand, the corroded sample, taken from the hot face shows a higher irreversible expansion up to 800 °C. Creep is observed above this temperature [9]. These experimental results demonstrate a relationship between corrosion and volume change which contributes to generating internal stresses in the tiles.

Table 1
Characteristics of SiC tiles.

Composition (wt %)		Physical properties	
SiC	90	Bulk density	2650 kg/m^3
SiO_2	8	Open porosity	15%
Al_2O_3	2.5	Cold crushing strength	110 MPa
Fe_2O_3	0.2	Thermal conductivity at 1100 °C	13 W/mK

The chemical composition of the deposit on the hot face of silicon carbide tile, determined after a lixiviation test (in water for 24 h), shows high contents of alkalis and calcium (Fig. 4). Moreover, the presence of a high amount of sulfur after lixiviation indicates that most of the deposit contains sulfate species.

Examinations of SiC samples, representative of the corrosive conditions, have been performed using X-ray diffraction (D8 Bruker advance diffractometer with Cu Kα radiation and a Vantec linear detector), scanning electron microscopy (FEI ESEM XL 40) and energy-dispersive X-ray spectroscopy (EDS).

The microstructure of an uncorroded brick has been studied by SEM (Fig. 5). This brick is composed of alpha-SiC aggregates and a rich silico-aluminate matrix containing some impurities such as lime (Table 2).

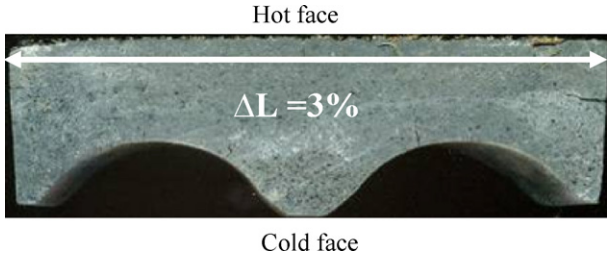

Fig. 2. Cross section of brick after use in an industrial waste incineration plant.

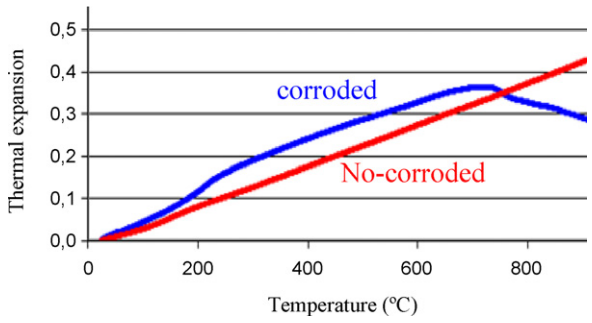

Fig. 3. Thermal expansion performed on uncorroded and corroded tile.

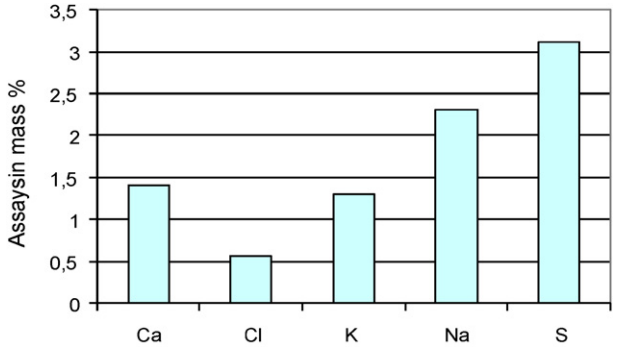

Fig. 4. Chemical composition of the deposit after lixiviation test.

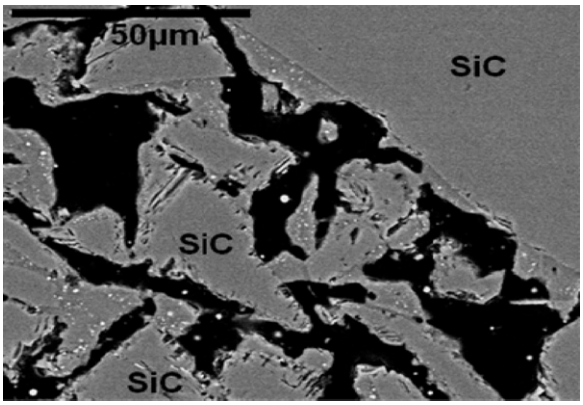

Fig. 5. Microstructure of uncorroded SiC tile (SEM backscattered electrons micrograph.

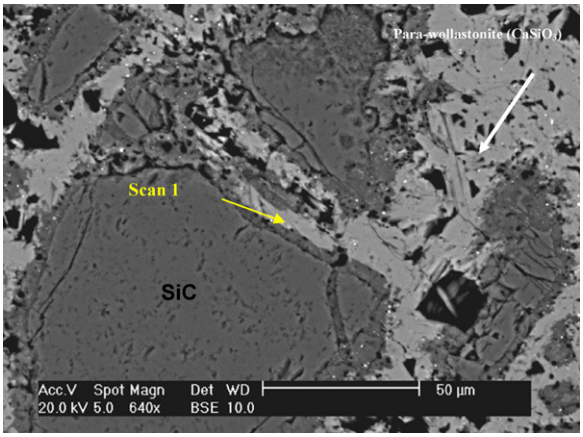

Fig. 6. Microstructure of corroded SiC tile at 5 mm from hot face (SEM backscattered electrons micrograph).

Regarding the corroded tiles, a new phase formed in the porosity of the sample appears on the hot face (Fig. 6). The chemical composition of this phase (Table 3) and the XRD performed on the hot face shows that para-wollastonite

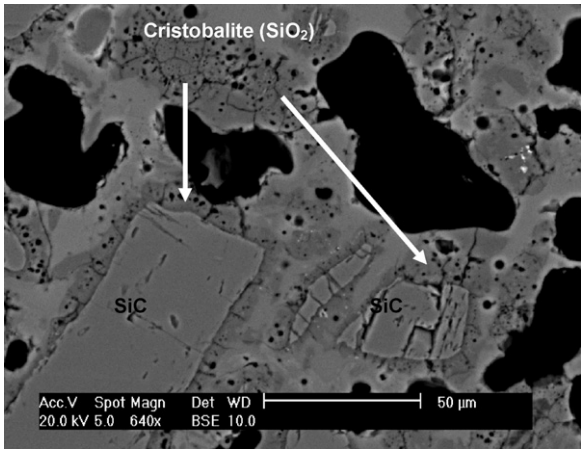

Fig. 7. Microstructure of corroded SiC tile at 20 mm from hot face (SEM backscattered electrons micrograph).

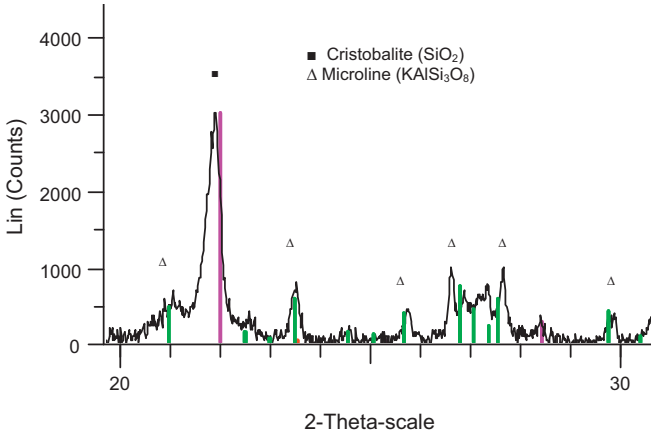

Fig. 8. Diffractogram performed in the middle of SiC refractory sample (20–30 mm from the hot face).

($CaSiO_3$) has crystallized. Around the SiC grains, a silica layer is observed due to the oxidation of SiC. Halfway through the thickness of the sample (Fig. 7), cristobalite is formed around the SiC grains due to their oxidation and microline ($KAlSi_3O_8$) was detected by X-ray diffraction (Fig. 8) and by EDS analysis (Table 4). On the cold face, the microstructure was similar to an uncorroded material.

Table 5 gives the chemical composition of the matrix before and after corrosion: the increase in alkalis in the matrix is very important (>10 wt% of K_2O). A global analysis, of 2 mm by 1.2 mm zones, including SiC aggregates and matrix, has been performed by EDS. Fig. 9 shows the evolution of the oxide contents from the hot face (distance = 0 mm) to the middle of the tile (distance = 30 mm).

Table 2
Chemical composition of the bonding of SiC tile performed by EDS.

Oxides	Na_2O	MgO	Al_2O_3	SiO_2	K_2O	CaO	TiO_2
wt%	0.15	0.7	20.9	73.4	0.7	3.1	0.15

Table 3
EDS analyses of the Fig. 6.

Elements wt%	Scan 1	Scan 2
O	53.6	43.9
Mg		0.4
Si	44.6	23.6
S	0.5	
Ca	0.45	31.3
Fe		0.8

Table 4
EDS analyses of the Fig. 7.

Elements (wt%)	Scan 1	Scan 2	Scan 3	Scan 4
O	50.81	53.48	49.62	51.19
Na			1.67	1.84
Al			4.80	5.61
Si	48.79	45,9	34.35	30.84
S	0.40	0.52	0.24	0.74
K			7.35	7.80
Ca				0.49
Fe			1.97	1.32

3. Thermodynamic simulation

Several authors [10,11] have calculated the condensed species as a function of the temperature and have found the formation of sulfate and chloride species in most cases, especially with Ca, K and Na elements.

Based on the elementary composition of household waste, thermo-chemical calculations were performed by FactSage© (version 6.1) in order to have a better understanding of species reacting with refractory. The associated databases used in this study were: ELEM (elements thermodynamic database), FACT 53 (gas species, solid and liquid compounds thermodynamic database), and FT-oxid (compounds and solutions for oxides database).

The thermodynamic simulation was based on the post mortem examination of oxide bonded silicon carbide refractories. The corrosive species impregnate the tile more or less,

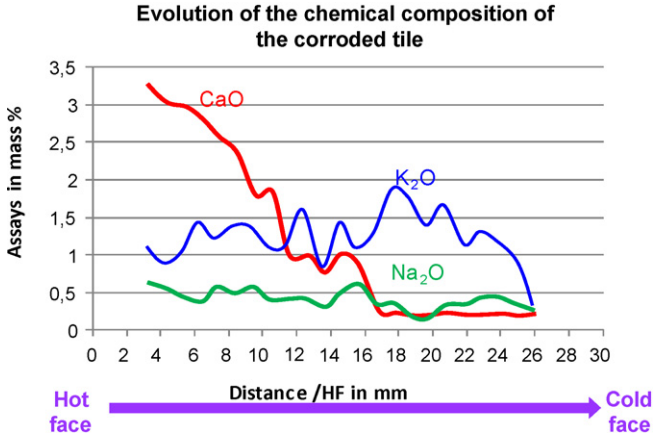

Fig. 9. Evolution of oxides content in corroded tile.

Table 5
Evolution of chemical composition (wt%) of matrix in uncorroded and corroded title.

Oxides (wt%)	Matrix of uncorroded brick (Fig. 3)	Matrix of corroded brick (Fig. 6)
Na_2O	0.1	2.7
MgO	0.5	0.0
Al_2O_3	14.8	12.2
SiO_2	81.0	72.9
K_2O	0.4	10.3
CaO	3.0	0.8
TiO_2	0.1	0.0
S	0.0	0.7

condense or not, and can react with the host material. The temperature of the condensed species in the tile depends obviously on the temperature of the tile, which varies through the thickness. The thermo-chemical reactions will depend on the existing species and the thermal gradient. The calculations were carried out, the temperature decreasing step by step from an initial value. At each new step, only the gas species formed at the previous step, limited to those with a concentration above 1×10^{-6} mol, were input to determine the condensed species for the current temperature. The iterative computation was performed until there was no more new formed solid or liquid species.

The temperature of waste combustion ranges from 1100 to 1200 °C. Therefore, the initial temperature was fixed at 1150 °C. As mentioned above, the initial species were determined from the composition of European usual household waste [12] and it is worth noting that thermo-chemical results depend strongly on the initial composition. Gaseous, liquid and solid species able to react with the refractory were then calculated from the initial chemical composition of the waste (Table 6). Necessary air for the self-combustion was injected as well.

Regarding the iterative computation, the temperature step was 50 °C. The simulation shows no more new condensed species formed below 550 °C.

The temperature distribution of the tiles (Fig. 10) was determined by thermal modeling with Abaqus FEA software.

Table 6
Input data used for the thermodynamic calculations.

Elements	mol/kg waste
C	32.22
H	61.51
O	17.44
N	0.93
S	0.06
Cl	0.16
Ca	0.77
K	0.13
Na	0.30
Al_2O_3	0.59
SiO_2	2.55
H_2O (steam)	27.75
Air combustion (m^3/kg)	5
N_2 (79% m)	176.34
O_2 (21% m)	46.88

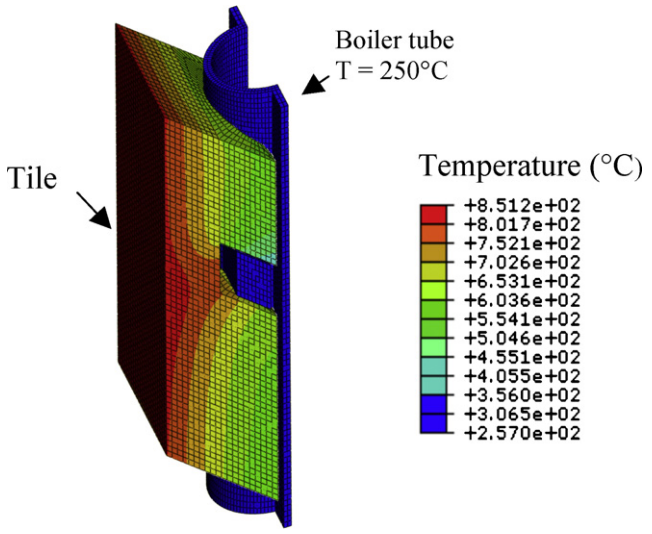

Fig. 10. Temperature range of a tile in service condition (Abaqus software).

The temperature of flue-gas, the heat transfer coefficient of the refractory and the design of the tile [13] were taken into account (Fig. 11).

The temperature ranged from 800 to 850 °C on the hot face and decreased to 600 °C on the cold face in contact with boiler tube. The numerical results were validated thanks to temperature data measured by thermal couples placed inside the tiles during service.

The species condensed at 1150 °C and between 850 °C and 650 °C are presented in Fig. 12. Calcium element is condensed only at high temperature as oxide and sulfate compounds. The condensation of alkali sulfates occurs between 850 °C and 550 °C. However, the experimental data given by the literature [10,14] are not totally in accordance with the thermo-chemical modeling. This can be explained by the fact that the lime can react with the chloride acid contained in the gas mixture to form calcium chloride species at high temperatures under optimal conditions. At lower temperature, calcium chloride species

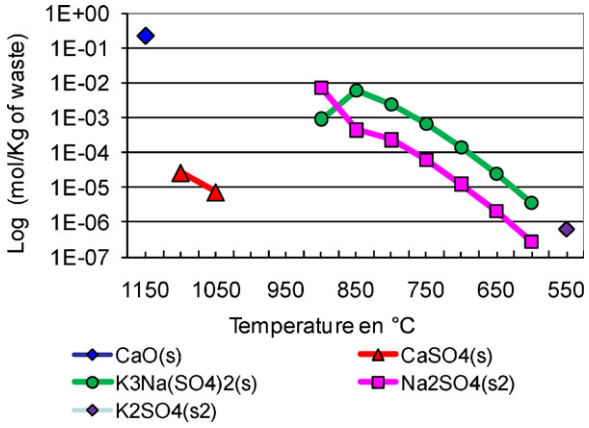

Fig. 12. Species condensed at a temperature range of 1150–550 °C.

react then with oxide sulfur to form calcium sulfate following the reaction (1):

$$CaCl_2(g) + SO_2(g) + ½O_2 + H_2O \rightarrow CaSO_4(s) + 2HCl(g) \quad (1)$$

Thus, in actual conditions, calcium sulfate can form and condense at lower temperatures, which corresponds to the temperature of the refractory lining (850 °C).

The phases obtained by the iterative thermo-chemical simulation at different temperatures depend on the initial composition (% in mass of Si, Al, Ca, K and Na) but also the composition of selected gas species. Thus, in some cases, gaseous NaCl and KCl can be condensed into solid species between 850 °C and 600 °C [11].

4. Discussions

Several authors described the formation of gaseous chlorine species (HCl, Cl_2) during the sulfation of KCl, NaCl and $CaCl_2$ [15,16].

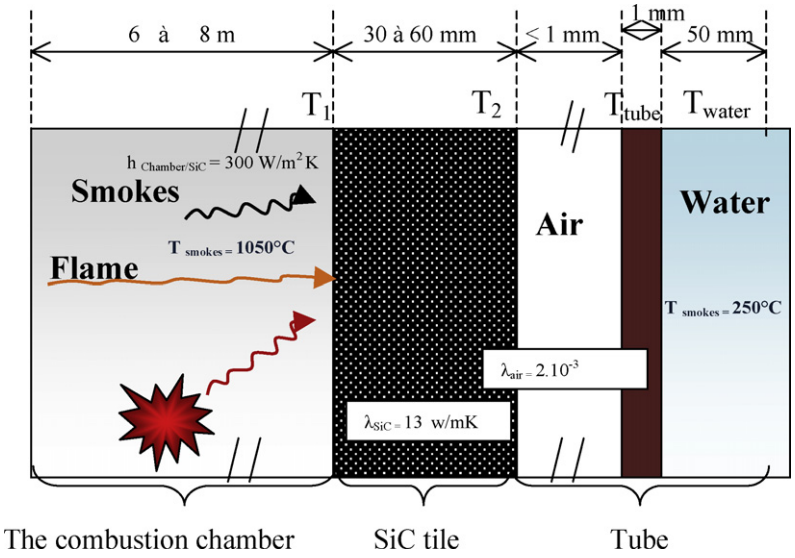

Fig. 11. Scheme of heat transfer in the refractory lining.

The following reactions related to the formation of HCl and Cl_2 from inorganic chlorides, were considered for thermodynamic calculations:

$$MCl_X(g) + (x/2)SO_2(g) + x/4O_2(g) + (x/2)H_2O(g) \rightarrow (x/2)M_{(2/x)}SO_4(s) + xHCl(g) \quad (2)$$

where M represents the metal elements (Ca, Na or K) and x the stoechiometric coefficient.

Thus, sulfation of chlorides depend on the metal elements, the temperature, the partial pressure of oxygen and the water vapor content.

In addition, the oxidation of SiC is accelerated by the H_2O content [17,18]. In the combustion chamber, the atmosphere contains 30 wt% of H_2O. The main reaction is the following:

$$SiC(s) + 3H_2O(g) \rightarrow SiO_2(s) + CO(g) + 3H_2(g) \quad (3)$$

Other authors described the mechanism of corrosion of SiC by molten salts and especially by Na_2SO_4 [6,7,19].

In the presence of O_2, it appears that $Na_2SO_4(l)$ dissolves the oxide film layer to form liquid sodium silicate following the reactions:

$$Na_2SO_4(l) = Na_2O(s) + SO_3(g) \quad (4)$$

$$SO_3(g) = SO_2(g) + ½O_2(g) \quad (5)$$

$$Na_2O(s) + 2SiO_2(s) = Na_2Si_2O_5(l) \quad (6)$$

Na_2O can also be formed from the reaction of NaCl with water vapor [20].

Thus, the corrosion mechanisms are linked to two phenomena:

- The first reaction is related to the condensation of calcium sulfate and alkali compounds (sulfates and chlorides) on the hot face of the refractory lining which forms a low eutectic point and reacts with the silica present in the matrix and the SiC grains.

Acidity is defined by pH in aqueous medium [21] while it is defined by $p(O_2-) = -\log(O_2^-)$ in molten salts.

An oxo-base is a donor of O_2^- ions (SO_4^{2-}, SiO_3^{2-}, MgO, CO_3^{2-} etc.) and an oxo-acid is an acceptor of O_2^- ions ($S_2O_7^{2-}$, SiO_2, Mg^{2+}, CO_2 etc.).

During corrosion, SiC may undergo passive oxidation to form silica [22,23]. In this case, sulfates are oxo-bases and give O_{2-} ions in the molten salts medium. These ions react with the silica (oxo-acid) following the reactions:

$$SO_4^{2-} \rightarrow SO_2 + O^{2-} \quad (7)$$

$$SiO_2 + O^{2-} \rightarrow SiO_3^{2-} \quad (8)$$

The SiO_3^{2-} ions react then with Ca^{2+} cations from the dissociation of calcium sulfate at high temperature to form para-wollastonite ($CaSiO_3$) following the reaction:

$$SiO_3^{2-} + Ca^{2+} \rightarrow CaSiO_3 \quad (9)$$

- The second reaction is linked to a condensation of alkali sulfate species into the porosity of refractory at a depth depending on the thermal gradient.

Na and K included in the molten salts penetrate into the network-formers (matrix) as a network modifier. The presence of alkalis leads to the formation of cristobalite around the SiC grains and in the matrix at lower temperatures. Indeed, experiments of K. Tomita et al. [24] on the mineralization effects of KCl and NaCl on the transformation of amorphous silica have shown that the SiO_2 crystallizes into cristoballite at 600 °C. The high potassium amount in the alumino-silica matrix can form microline ($KAlSiO_8$).

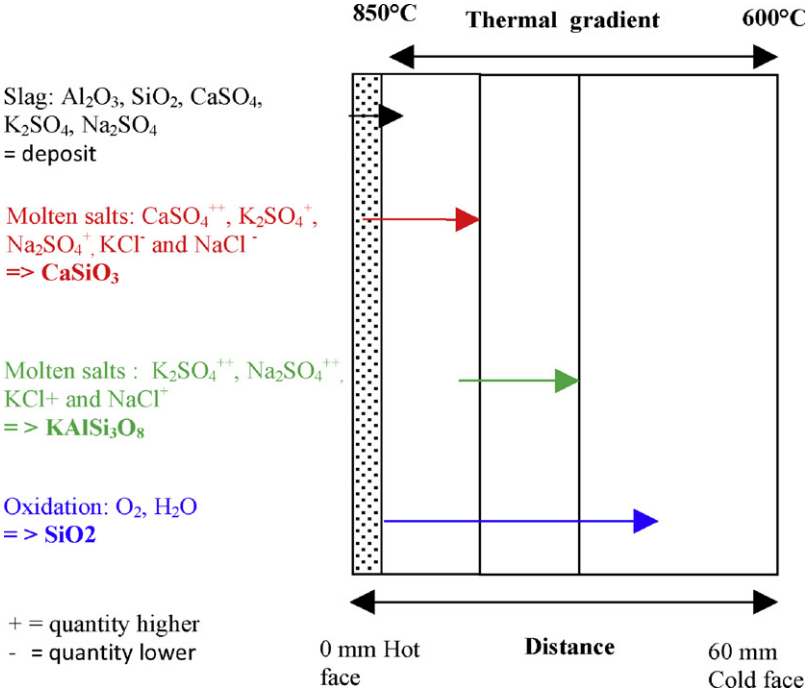

Fig. 13. Corrosion mechanisms in oxide bonded silicon carbide tiles.

Fig. 13 summarizes the corrosion mechanisms occurring in the refractory tile. Finally, it seems that the refractory damage induced by corrosion can be explained in two ways. On the one hand the oxidation of SiC is related to a volume expansion due to the difference of the molar volumes between SiC and SiO_2, thereby inducing high stresses [25,26]. Moreover, the higher thermal expansion of the formed cristobalite than that of amorphous silica may lead to tensile stresses and cracking in the refractory [27].

On the other hand, the crystallization of the para-wollastonite in the whole porosity on the hot face of the refractory tile, with a thermal expansion ($7–8 \times 10^{-6}/°C$) [28] coefficient higher than that of SiC ($5 \times 10^{-6}/°C$), may lead to severe mechanical damage as well.

5. Conclusion

In this research, the SEM observations of corroded oxide bonded silicon carbide refractories have shown a microstructural change due to corrosion by gaseous species.

Indeed, gaseous alkali species are involved, not only in the formation of liquid phases, but also as a precursor of cristobalite formation. It appears that cristobalite may crystallize from the silica layer around the SiC grains due to their oxidation as well as in the rich alumina-silica matrix.

On the hot face of the refractory, the main result is that the reaction chain based on oxo-reduction reactions produces para-wollastonite. The result is bulging due to mineral phases changes, which can cause the deformation of several zones in the incinerator. All results suggest two axes of improvement:

- A material way by a modification of the matrix: particularly the reduction of the porosity, the use of mullite or Si_3N_4 matrix, and/or the addition of a protective layer on the hot face;
- A technical way by a modification of the isotherms of the tiles. Reducing the temperature on the hot face should avoid the condensation of sulfate species in the porosity of materials.

Acknowledgments

The authors thank ANR (Agence Nationale de la Recherche, France) and the MATETPRO (Programme Matériaux et Procédés) for their helpful financial contribution in this research.

References

[1] N. Schmitt, A. Burr, Y. Berthaud, J. Poirier, Micromechanics applied to the thermal shock behavior of refractory ceramics, Mechanics of Materials 34 (2002) 725–747.
[2] E. Blond, N. Schmitt, F. Hild, P. Blumenfeld, J. Poirier, Effect of slag impregnation on thermal degradations in refractories, Journal of American Ceramic Society 90 (1) (2007) 154–162.
[3] D.W. McKee, D. Chatterji, Corrosion of silicon carbide in gases and alkaline slag, Journal of American Ceramic Society 59 (9) (1976) 9–10.
[4] N.S. Jacobson, Corrosion of silicon-based ceramics in combustion environments, Journal of American Ceramic Society 76 (1) (1993) 3–28.
[5] H.P. Nielsen, F.J. Frandsen, K. Dam-Johansen, L.L. Baxte, The implications of chlorine-associated corrosion on the operation of biomass-fired boilers, Progress in Energy and Combustion Science 26 (3) (2000) 283–298.
[6] S.N. Jacobson, J.L. Smialek, Hot corrosion of sintered α-SiC at 1000 °C, Journal of American Ceramic Society 68 (8) (1985) 432–439.
[7] M.K. Ferber, J. Ogle, V.J. Tennery, T. Henson, Characterization of corrosion mechanisms occurring in a sintered SiC exposed to basic coal slags, Journal of American Ceramic Society 68 (4) (1985) 191–197.
[8] J. Poirier, M.L. Bouchetou, F. Qafssaoui, J.P. Ildefonse, Analysis and interpretation of refractories microstructures in studies of corrosion mechanisms by liquid oxides, Journal of European Ceramic Society 28 (8) (2008) 1557–1568.
[9] E. Blond, N. Schmitt, F. Hild, P. Blumenfeld, J. Poirier, Modeling of high temperature asymmetric creep behavior of ceramics, Journal of European Ceramic Society 25 (2005) 1819–1827.
[10] D.O. Albina, K. Millrath, N.J. Themelis, Effects of feed composition on boiler corrosion waste-to-energy plants, in: 12th North American Waste To Energy Conference (NAWTEC 12), Savannah, Georgia, USA, May 17–19, 2004, pp. 1–11.
[11] N. Otsuka, Y. Nishiyama, Thermodynamic equilibrium calculations of deposits on superheater tubes in waste incinerations, paper no. 00229, Corrosion 2000, Orlando, USA, March 26–31, 2000.
[12] J. Manders, Life cycle assessment of the treatment of MSW in the average European Waste To Energy plant http://www.cewep.com, in: Confederation of European Waste-to-Energy Plants, 4th CEWEP Congress, June 12, 2008.
[13] P. Prigent, Multi scale approach of high temperature corrosion mechanisms of ceramic refractories, Ph.D. Thesis, University of Orléans, France, 2010.
[14] P. Radmakers, W. Hesseling, J. Van De Wetering, Review on corrosion in waste incinerators and possible effect of bromine, TNO Industrial Technology report, I02/01333/RAD, 2003, 1–51.
[15] H. Matsuda, S. Ozawa, K. Naruse, K. Ito, Y. Kojima, T. Yanase, Kinetics of HCl emission from inorganic chlorides in simulated municipal wastes incineration conditions, Chemical Engineering Science 60 (2) (2005) 545–552.
[16] M. Henriksson, B. Warnqvist, Kinetics of formation of HCl(g) by the reaction between NaCl(s) and SO_2, O_2 and H_2O(g), Industrial Process Design and Development 18 (1979) 249–254.
[17] E. Opila, The oxidation kinetics of chemically vapour deposited silicon carbide, in: TMS Fall Meeting, Chicago, 1992.
[18] P.J. Jorgensen, M.E. Wadsworth, I.B. Cutler, Effects of water vapour on oxidation of silicon carbide, Journal of American Ceramic Society 4 (6) (1961) 258–261.
[19] T. Hatta, K. Kuroda, H. Tsuda, Refractory attack by acid and alkali in municipal and industrial waste incinerators, Taikabutsu Overseas 8 (3) (1998) 32–43.
[20] M.J. Mc Nallan, M. van Roode, J.R. Price, The mechanism of high temperature corrosion of SiC in flue gases from aluminium remelting furnaces, Ceramics Transactions 10 (1990) 181–191.
[21] H. Flood, T. Förland, Acta Chemica Scandinavica 1 (1947) 592.
[22] M. Thorley, R. Banks, Kinetics and mechanism of oxidation of silicon nitride bonded silicon carbide ceramic, Journal of Thermal Analysis 42 (1994) 811–822.
[23] A. Gallet-Doncieux, O. Bahloul, C. Gault, M. Huger, T. Chotard, Investigations of SiC aggregates oxidation: influence on SiC castables refractories life time at high temperature, Journal of European Ceramic Society 32 (2012) 737–743.
[24] K. Tomita, M. Kawano, Effect of cations on crystallization of amorphous silica. II, Kagoshima Daigaku Rigakubu kiyo, Chigaku Seibutsugaku 26 (1993) 1–16.
[25] E. Mazzucato, A.F. Gualtieri, Wollastonite polytypes in $CaO–SiO_2$ system – Part 1 – Crystallization kinetics, Physics and Chemistry of Minerals 27 (8) (2000) 565–574.
[26] O. Bahloul, T. Chotard, M. Huger, C. Gault, Young's modulus evolution at high temperature of SiC refractory castables, Journal of Materials Science 45 (2010) 3652–3660.
[27] N.B. Pilling, R.E. Bedworth, The oxidation of metals at high temperatures, Journal of the Institute of Metallics 29 (1923) 529–591.
[28] Y.S. Touloukian, R.K. Kirby, R.E. Taylor, T.Y. Lee, Thermal expansion of non-metallic solids, Thermophysical Properties of Matter, vol. 13, IFI/Plenum, New York, 1970.